Received: 2 May 2021 | Revised: 24 July 2021 | Accepted: 7 August 2021

IET Generation, Transmission & Distribution

DOI: 10.1049/gtd2.12270

The Institution of Engineering and Technology WILEY

ORIGINAL RESEARCH PAPER

Adaptive robust optimal dispatch of microgrid based on different robust adjustment parameters

Jun Yang | **Changqi Su** | **Zhiliang Wang**

College of Information Science and Engineering, Northeastern University, Shenyang, China

Correspondence
Jun Yang, No.134 Mailbox, College of Information Science and Engineering, Northeastern University, Shenyang, 110819, China.
Email: yangjun@mail.neu.edu.cn

Funding information
National Key R&D Program of China, Grant Number: 2018YFA0702200; National Natural Science Foundation of China, Grant Number: 61773099

Abstract

This paper proposes a microgrid adaptive robust optimal dispatch model with different robust adjustment parameters to improve the operating economy and safety of large-scale renewable distributed energy integration into the microgrid system. Through a robust equivalent process, considering the uncertain characteristics of the renewable energy output and load demand in the microgrid, the uncertain parameters are converted into corresponding definite parameters. A two-stage robust optimization model is established to minimize the operating cost of the microgrid under the premise of ensuring the robustness of the microgrid. An improved Benders algorithm is proposed to solve the established optimization model. The different robust adjustment parameters can be obtained adaptively through the optimization program. The optimized adaptive robust adjustment parameters can better reflect the balance between the economy and robustness of the microgrid operation, and are more suitable for the operation of the microgrid. The improved Benders algorithm can effectively speed up the solution and improve the efficiency of the solution. The simulation of the modified IEEE39-bus system verifies the rationality of the proposed optimization model and the advantages of the improved algorithm.

1 | INTRODUCTION

The severe situation of global climate change and fossil fuel pollution prevention has promoted the rapid development of renewable energy. Renewable energy has the advantages of clean, pollution-free and sustainable supply, but it also has unfavourable factors such as intermittency and volatility, which brings great challenges to the safe and stable operation of the energy system [1]. With the further increase in the proportion of renewable energy, the penetration rate of renewable energy in some areas has exceeded 100%, reflecting the characteristics of a completely renewable energy system. However, due to insufficient local absorption capacity, it is easy to cause serious failures, such as power reverse transmission and voltage overrun [2], which pose a great threat to the safe and stable operation of the power grid. This in turn leads to phenomena such as 'abandonment of wind' and 'abandonment of solar', which reduce the economics of renewable energy.

As one of the effective ways to connect distributed power sources to the grid, microgrids have also received extensive attention. A microgrid is a small power generation and distribution system that integrates distributed power, energy storage, and loads [3]. Through the coordination and collaboration of internal sources and load storage units, the microgrid can realize autonomous operation and friendly grid-connected interaction. It is an effective carrier for large-scale distributed renewable energy to connect to the grid [4].

As a core technology of microgrid, optimal dispatching of the microgrid is an important support to deal with the uncertainty of renewable energy and load and ensure the economic and reliable operation of the microgrid [5, 6]. Regarding the optimal dispatch of microgrids, a large number of references have been studied. According to the optimization goals, the optimal dispatch of microgrids can be divided into microgrid-level optimization, demand-side response-level optimization and distribution network-level optimization [7]. The optimal dispatch method of microgrid needs to be based on the prediction of uncertain factors. Many statistical models and physics-based methods have been used to predict renewable distributed energy, such as autoregressive moving average models [8] and

artificial neural networks [9, 10]. Although wind power forecasting, photovoltaic power generation forecasting and load forecasting technologies have become increasingly mature, accurate forecasting is still a difficult task. According to the optimization method, the optimization dispatch method of microgrid can be divided into deterministic method and uncertainty method.

The deterministic method takes the predicted value of renewable distributed power as an accurate known quantity and then optimizes the dispatch of the microgrid. The rolling view strategy is applied to the mixed integer nonlinear programming model to optimize the operation of multiple buildings in the microgrid in a centralized manner [11], aiming to solve the data uncertainty problem by reducing the amount of forecast data required. Reference [12] proposed a two-stage mixed integer linear programming model based on 24-hour advance forecast data to reduce the operating cost of microgrids. This deterministic method does not consider the uncertainty of the prediction parameters, which will bring bias to the optimization results.

Aiming at the uncertainty method in the optimization and dispatching of microgrid operations, the main solutions in existing research include spinning reserve capacity [13], stochastic planning [14], scenario analysis [15], and robust optimization [16]. Regarding spinning reserve capacity, related research is mainly to optimize spinning reserve capacity so that it can invest in the smallest capacity and achieve an economically optimal operation effect [17]. A simple and effective optimization method is a major advantage of using the spinning reserve capacity method to solve uncertain problems [18]. However, the solution to the spinning reserve capacity method is that sufficient reserve capacity is needed to deal with uncertain problems, and the corresponding reserve capacity will increase the operating cost of the microgrid. Stochastic planning is a common method to solve the uncertain problem of microgrids, which need to be optimized according to the probability distribution of uncertain parameters [19]. However, the probability distribution of uncertain parameters is difficult to accurately describe and may cause errors in the optimization results. It is difficult to accurately determine the probability distribution, which also hinders the application of stochastic programming. The scenario analysis method generates typical scenarios through scenario generation and scenario reduction [20], and optimizes the microgrid according to the typical scenarios. The generation of the scene tree will produce high-dimensional and complex operations, resulting in a problem of low solution efficiency. Scene reduction will also cause the problem of reduced solution accuracy [21].

Compared with other uncertain methods, robust optimization has the following advantages. Robust optimization does not need to know the specific probability distribution function of the uncertainty parameter, and only needs to know the boundary information to construct an optimization model containing the uncertain parameter [22]. The optimization results obtained by the robust optimization method are robust. When the uncertain factors fluctuate within the set range, the optimization results can ensure the stability and feasibility of the system.

Robust optimization methods have been applied to many types of research on microgrids. Aiming at the frequency deviation problem caused by the volatility of renewable distributed energy and load demand, reference [23] proposed a two-stage robust optimization model to ensure the flexible operation of the microgrid. A variety of robust optimization methods are used for the optimal dispatch control problem of the microgrid energy storage system. The robust optimization method combined with the piecewise linearization technology of the nonlinear efficiency graph ensures robustness in terms of reducing operating costs and accurate calculations [24]. For integrated energy systems and multi-microgrid systems, robust optimization is still widely used. In order to cope with the microgrid optimization scheduling problem of combined cooling, heating, and power (CCHP), reference [25] applies a coordinated adaptive robust optimization method with multiple time scales to optimize microgrids with multiple different energy types. A stakeholder-parallel adaptive robust optimization model is proposed in [26], which is used to solve the optimal dispatching problem among multiple microgrids.

Robust optimization is more applied to the research of optimal dispatching of the microgrid. Reference [27] proposed a resource cost-constrained adaptive robust optimization model with binary resource variables to solve the problem of optimal scheduling of source and load uncertainties. A distributed robust optimization method is to combine stochastic programming and robust optimization to find the worst-case probability distribution on the fuzzy sets [28], and use the fuzzy set to represent the uncertain variables in the sub-Brussels optimization model, and finally get the lowest operating costs in the worst case. Reference [29] proposes a microgrid energy management system based on robust convex optimization, which is used to solve the energy optimization management problem of a microgrid when the random load demand is large and the renewable energy supply is insufficient. Reference [30] solves the uncertainty problem in the microgrid from the perspective of load response and is based on price demand response. Compared with other methods of dealing with uncertain problems, robust optimization has obvious advantages. However, the traditional robust optimization method used in the above-mentioned research is based on the worst-case scenario of uncertain factors to carry out the economic optimization operation of the microgrid. So, it can ensure that the microgrid has sufficient robustness. But, this method will inevitably cause the problem of too conservative optimization results, increase the operating cost of the microgrid, and cannot guarantee the economics of microgrid operation. Aiming at the problem that traditional robust optimization methods are too conservative, a robust optimization method based on historical correlation drive (HCD) to formulate interval boundaries is proposed in [31]. Although the HCD robust optimization method can avoid unreasonable scenarios, it still cannot discuss the economy and robustness of microgrid operation at the same time. Reference [32] proposes a robust mixed integer second-order cone programming model, but the established optimization model is only proposed for microgrid operation in island mode. Considering the

economy and robustness of microgrid operations, reference [33] uses robust equivalent characterization to deal with uncertain factors. However, using the same robust adjustment parameter processing for different uncertain factors will still lead to a conservative solution. Reference [34] uses the uncertainty factor budget method to deal with the wind power uncertainty and achieve a robust optimization operation solution for the microgrid with a natural gas network. However, more uncertainties should be considered.

In view of the above-mentioned problems, this paper proposes an adaptive robust optimization model for a microgrid with different robust adjustment parameters, which can effectively take into account the balance of economy and robustness of microgrid operation. The main contributions to this work are summarized as follows:

1. The adaptive multi-parameters robust equivalent characterization method is used to convert uncertain parameters into definite adjustable parameters. The robust adjustment parameters in the multi-parameters robust equivalent representation can be adaptively obtained through the optimization program, which conforms to the characteristics of uncertain factors.
2. The robust adjustment parameters are obtained by an optimization procedure, so that the optimal dispatch of the microgrid can adaptively adjust the robustness of uncertain factors. The proposed robust adjustment parameters can reflect the balance between economy and robustness better, which are most suitable for microgrid operation.
3. The established robust optimization model is suitable for the two operating modes, grid-connected mode and island mode respectively. The optimization model proposed in this paper has better applicability, which is more in line with engineering needs.
4. The established robust optimization model adopts the structure of Min-max-min, which can be solved by the improved Benders algorithm. The improved Benders algorithm uses acceleration parameters ς in the constraints of the main problem to increase the lower limit of the original problem. The proposed improved Benders dual algorithm can speed up the solution process and improve the solution efficiency as shown in the simulation.

The rest of this paper is organized as follows. The microgrid system structure is given in Section 2. Robust equivalent representations with different robust adjustment parameters are given in Section 3. The adaptive robust optimization model of the microgrid is presented in Section 4. Section 5 proposes an improved Benders algorithm to optimize the optimization model. Simulation and analysis are given in Section 6. The conclusion is given in Section 7.

2 | MICROGRID SYSTEM STRUCTURE

The content of this paper is the optimization of the microgrid in grid-connected mode and island mode. When the microgrid is connected to the grid, the surplus power of the microgrid can be traded to the main network, and the shortfall power of the microgrid can also be purchased from the main network. When the microgrid operates in island mode, there is no power interaction between the microgrid and the main grid, and the microgrid can only achieve a balance of energy supply and demand among its internal units. The microgrid studied in this paper includes traditional distributed power sources, renewable distributed power sources, energy storage systems, and loads. Among them, traditional distributed power sources include micro gas turbines, and renewable distributed power sources include wind generators and photovoltaic power sources.

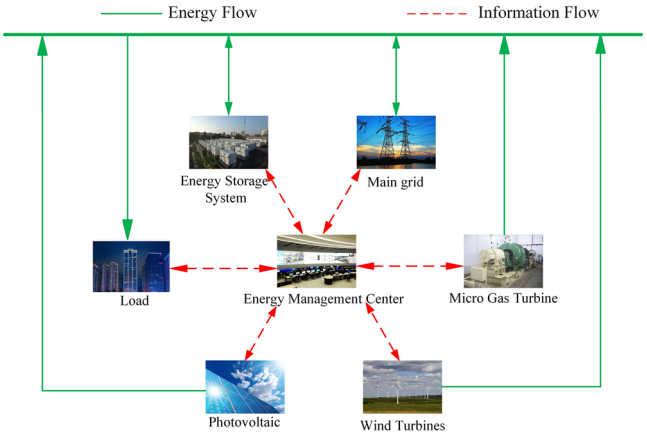

FIGURE 1 Schematic diagram of microgrid system structure

The schematic diagram of the microgrid system structure is shown in Figure 1. Among them, there is only information flow interaction between the energy management centre and each unit of the microgrid. Based on the historical power generation data and load historical usage data of the renewable distributed power sources, the energy management centre predicts the forecast data of the microgrid renewable distributed power output and load demand in the next time period. The energy management centre then performs robust optimization calculations based on the predicted data, and obtains an optimized dispatching plan for the microgrid in the scenario with the smallest operating cost of the microgrid, and completes the optimized dispatch of the microgrid.

3 | ROBUST EQUIVALENT CHARACTERIZATION OF UNCERTAIN PARAMETERS

The robust equivalent characterization of uncertain parameters proposed in this paper includes the robust equivalent characterization of renewable energy power generation and the robust equivalent characterization of load demand. Renewable energy power generation includes photovoltaic power generation and wind power generation.

3.1 | Robust equivalent characterization of photovoltaic power output

Assume that the probability density function of photovoltaic output obeys the Beta distribution, as shown in Equation (1):

$$p_{p,t}^{PV} \sim \text{Beta}(\alpha_{p,t}, \beta_{p,t}) \tag{1}$$

where $p_{p,t}^{PV}$ is the probability density function of the photovoltaic generator set on node p in the time period t. $\alpha_{p,t}$ and $\beta_{p,t}$ are the two parameters of the Beta distribution respectively. Among them, $\alpha_{p,t}$ is the shape parameter of photovoltaic output, and $\beta_{p,t}$ is the rate of photovoltaic output.

However, the probability density of photovoltaic output does not accurately represent the photovoltaic output, and there are errors. Therefore, the probability density of photovoltaic output needs to be adjusted. The robust equivalent characterization process of photovoltaic output is shown in Equations (2) and (3):

$$P_{p,t}^{PV} = \text{CDF}_{p,t}^{-1}\left(\tilde{P}_{p,t}^{PV} - \zeta_{PV}\right) \quad \forall p \in \Omega_{PV} \tag{2}$$

$$\tilde{P}_{p,t}^{PV} = \int_{-\infty}^{E_{PV,t}} p_{p,t}^{PV}\,\text{dx} \tag{3}$$

where $P_{p,t}^{PV}$ is the robust equivalent characterization of photovoltaic output. $\text{CDF}^{-1}(\bullet)$ is the inverse function of the cumulative distribution function. $\tilde{P}_{p,t}^{PV}$ is the cumulative distribution function of photovoltaic output. ζ_{PV} is the robust adjustment parameter of photovoltaic output. Ω_{PV} is the collection of all nodes configured with photovoltaic power. $E_{PV,t}$ is the expectation of photovoltaic output, calculated based on photovoltaic output.

3.2 | Robust equivalent characterization of wind turbine output

Assuming that the probability density function of wind power output obeys the Weibull distribution, as shown in Equation (4):

$$p_{\omega,t}^{WT} \sim \text{Weibull}(\kappa_{\omega,t}, \lambda_{\omega,t}) \tag{4}$$

where $p_{\omega,t}^{WT}$ is the probability density function of the wind turbine output at a node ω in a time period t. $\kappa_{\omega,t}$ and $\lambda_{\omega,t}$ are the two parameters of the Weibull distribution respectively. Among them, $\kappa_{\omega,t}$ is the shape parameter of wind power output, and $\lambda_{\omega,t}$ is the scale of wind power output.

However, similar to the probability density of photovoltaic output, the probability density of wind power output cannot accurately represent the wind power output, and there are errors. Therefore, the probability density of wind power output needs to be adjusted. The robust equivalent characterization process of wind power output is shown in Equations (5) and (6):

$$P_{\omega,t}^{WT} = \text{CDF}_{\omega,t}^{-1}\left(\tilde{P}_{\omega,t}^{WT} - \zeta_{WT}\right) \quad \forall \omega \in \Omega_{WT} \tag{5}$$

$$\tilde{P}_{\omega,t}^{WT} = \int_{-\infty}^{E_{WT,t}} p_{\omega,t}^{WT}\,\text{dx} \tag{6}$$

where $P_{\omega,t}^{WT}$ is the robust equivalent characterization of the wind turbine output. $\tilde{P}_{\omega,t}^{WT}$ is the cumulative distribution function of wind turbine output. ζ_{WT} is the robust adjustment parameter of wind turbine output. Ω_{WT} is the set of all nodes configured with wind turbines. $E_{WT,t}$ is the expectation of the wind turbine output, calculated according to the wind turbine output.

3.3 | Robust equivalent characterization of load demand

Assuming that the probability density function of load demand obeys the normal distribution function, as shown in Equation (7):

$$p_{i,t}^{D} \sim N(\mu_{i,t}^{P}, \sigma_{i,t}^{P}) \tag{7}$$

where $p_{i,t}^{D}$ is the active power probability density function of the load demand of the node i in the time period t. $\mu_{i,t}^{P}$ and $\sigma_{i,t}^{P}$ are the average value and standard deviation of the active power demand of node i in a time period t.

Similarly, the probability density of load demand cannot accurately represent load demand because of errors. Therefore, the probability density of load demand needs to be adjusted. The robust equivalent characterization process of load demand is shown in Equations (8) and (9):

$$P_{i,t}^{D} = \text{CDF}_{i,t}^{-1}\left(\tilde{P}_{i,t}^{D} + \zeta_{D}\right) \quad \forall i \in \Omega_{D} \tag{8}$$

$$\tilde{P}_{i,t}^{D} = \int_{-\infty}^{E_{P,t}} p_{i,t}^{D}\,\text{dx} \tag{9}$$

where $P_{i,t}^{D}$ is the robust equivalent representation of the active power and reactive power of the load demand of a node i in the time period t. $\tilde{P}_{i,t}^{D}$ is the cumulative distribution function of the active power and reactive power of the load demand of a node i in the time period t. ζ_{D} is the robust adjustment parameter of load demand. Ω_{D} is a collection of all nodes configured with load. $E_{P,t}$ is the expectation of load active demand, which is calculated based on the load value.

3.4 | Robust adjustment parameters

The calculation methods of the robust adjustment parameters mentioned in Equations (2), (5) and (8) are as shown in

Equations (10), (11) and (12) respectively:

$$\zeta_{PV} = A * \mathrm{Y}_{PV} \tag{10}$$

$$\zeta_{WT} = A * \mathrm{Y}_{WT} \tag{11}$$

$$\zeta_{D} = A * \mathrm{Y}_{D} \tag{12}$$

where Y_{PV}, Y_{WT}, and Y_{D} are the adjustment coefficients of photovoltaic output, wind turbine output and load demand, and the value range is $0 < \mathrm{Y}_{PV/WT/D} < 1$. The calculation method of the parameter A is shown in Equations (13)–(15):

$$A = \min\left\{\underline{P},\ 1 - \bar{P}\right\} \tag{13}$$

$$\overline{P} = \max\left\{\tilde{P}^{D}_{i,t},\ \tilde{P}^{PV}_{p,t},\ \tilde{P}^{WT}_{\omega,t}\right\} \tag{14}$$

$$\underline{P} = \min\left\{\tilde{P}^{D}_{i,t},\ \tilde{P}^{PV}_{p,t},\ \tilde{P}^{WT}_{\omega,t}\right\} \tag{15}$$

Unlike the uncertainty parameters in [29] that use the same robust adjustment parameters, this paper uses different robust adjustment parameters to perform robust equivalent characterization of the uncertainty parameters. By optimizing different robust adjustment parameter values, the robust adjustment parameter values of uncertain parameters can be adaptively obtained respectively, so as to obtain the optimized scheduling result of microgrid operation better.

4 | ROBUST OPTIMIZATION MODELLING OF MICROGRID

4.1 | Objective function

The microgrid robust optimization model takes the microgrid operating cost as the optimization goal. The objective function is shown in Equation (16):

$$\min \sum_{t\in\Omega_T} \Delta_t \left\{ \left| \sum_{i\in\Omega} c^{ls}_i \left(\Psi_{i,t} P^{D}_{i,t}\right) + \sum_{b\in\Omega_{ESS}} \left(c^{ESS,dc}_b P^{ESS,dc}_{b,t} - c^{ESS,ch}_b P^{ESS,ch}_{b,t}\right) \right| + \max_{\zeta} \min \left(\sum_{i\in\Omega_S} c^{S}_t \Psi_S P^{S}_{i,t} + \left| \sum_{g\in\Omega_{DG}} c^{DG}_g P^{DG}_{g,t} + \sum_{p\in\Omega_{PV}} c^{PV}_p P^{PV}_{p,t} + \sum_{\omega\in\Omega_{WT}} c^{WT}_\omega P^{WT}_{\omega,t} \right| \right) \right\} \tag{16}$$

where Δ_t is the length of the time period within the optimization period t. c^{ls}_i is the unit load reduction cost at a node i. $\Psi_{i,t}$ is the binary variable related to load reduction in a node i in the time period t. When load reduction is required, $\Psi_{i,t} = 1$. When load reduction is not required, $\Psi_{i,t} = 0$. $c^{ESS,dc}_b$ is the unit discharge cost of the energy storage device at a node b. $P^{ESS,dc}_{b,t}$ is the discharge power of the energy storage device at the node b. $c^{ESS,ch}_b$ is the unit charging cost of the energy storage device at the node b. $P^{ESS,ch}_{b,t}$ is the charging power of the energy storage device at the node b. c^{S}_t is the unit cost of input power from the main network during a time t. Ψ_S is a 0–1 variable. $\Psi_S = 1$ indicates that the microgrid is in grid-connected mode. $\Psi_S = 0$ indicates that the microgrid is in island mode. $P^{S}_{i,t}$ is the power input by a node i from the main network during a time period t. c^{DG}_g is the unit cost of traditional distributed power generation at a node g. $P^{DG}_{g,t}$ is the generation power of the traditional distributed power supply at node g in the time period t. c^{PV}_p is the unit cost of photovoltaic power generation at a node p. c^{WT}_ω is the unit cost of wind turbines at the node ω. Ω is the set of all nodes included in the microgrid. Ω_{ESS} is the set of all nodes that configure the energy storage system. Ω_S is a set of nodes containing the point of common coupling (PCC). Ω_{DG} is a set of all nodes configured with traditional distributed power.

In (16), $c^{ls}_i\left(\Psi_{i,t} P^{D}_{i,t}\right)$ is the load shedding cost of the microgrid. $\left(c^{ESS,dc}_b P^{ESS,dc}_{b,t} - c^{ESS,ch}_b P^{ESS,ch}_{b,t}\right)$ is the charge and discharge cost of the energy storage system. $c^{S}_t \Psi_S P^{S}_{i,t}$ is the electricity interaction cost between the microgrid and the main grid. $c^{DG}_g P^{DG}_{g,t}$ is the cost of traditional distributed power supply. $c^{PV}_p P^{PV}_{p,t} + c^{WT}_\omega P^{WT}_{\omega,t}$ is the cost of renewable distributed power output, including photovoltaic costs and wind turbine costs.

4.2 | Constraints

The power flow constraint is an indispensable constraint in the microgrid. This paper establishes the power flow constraints of the microgrid through the DC power flow model, as shown in Equations (17)–(19). The establishment of DC power flow constraints in the microgrid is similar to the reference [33]. Equation (17) shows the power balance of the node. Equations (18) and (19) show the branch power flow constraint:

$$\Psi_S \sum_{i\in\Omega_S} P^{S}_{i,t} + \sum_{g\in\Omega_{DG}} P^{DG}_{g,t} + \sum_{b\in\Omega_{ESS}} \left(P^{ESS,dc}_{b,t} - P^{ESS,ch}_{b,t}\right) + \sum_{p\in\Omega_{PV}} P^{PV}_{p,t} + \sum_{\omega\in\Omega_{WT}} P^{WT}_{\omega,t} + \sum_{(i,j)\in\Omega_n} P_{(i,j),t} = \Psi_{n,t} P^{D}_{n,t} \tag{17}$$

$$B_{(i,j)}\left(\theta_{i,t} - \theta_{j,t}\right) - P_{(i,j),t} + \left(1 - \chi_{(i,j)}\right) M \geq 0 \tag{18}$$

$$B_{(i,j)}\left(\theta_{i,t} - \theta_{j,t}\right) - P_{(i,j),t} - \left(1 - \chi_{(i,j)}\right) M \leq 0 \tag{19}$$

where $P_{(i,j),t}$ is the active power of the corresponding DC power flow line (i, j) in the time period t. $P^{D}_{n,t}$ is the load of a node n at a time t. Ω_n is the set of lines connected to node n. $\Psi_{n,t}$ is the binary variable related to load reduction in a node n in a time period t. When load reduction is required $\Psi_{n,t} = 1$. When load reduction is not required, $\Psi_{n,t} = 0$. $B_{(i,j)}$ is the admittance of the corresponding DC power flow line (i, j). $\theta_{i,t}$ is the voltage phase angle of the node i. M is a sufficiently large positive value. When $\chi_{(i,j)} = 1$, the term contained M is 0, it is necessary to satisfy the branch tide constraints. When $\chi_{(i,j)} = 0$, the line is disconnected, the branch flow restriction does not work.

Since the microgrid system optimized in this paper contains traditional distributed power sources (micro gas turbine units), the constraints of traditional distributed power sources are also indispensable. The micro gas turbine unit constraints are shown in Equations (20)–(25) [29, 33]:

$$\left(P_{g,t}^{DG}\right)^2+\left(Q_{g,t}^{DG}\right)^2\le \Pi_{g,t}\left(\overline{S}_g^{DG}\right)^2 \tag{20}$$

$$P_{g,t}^{DG}\tan\left[\cos^{-1}\left(pf_g\right)\right]\ge Q_{g,t}^{DG} \tag{21}$$

$$R_g^{dw}\le P_{g,t}^{DG}-P_{g,t-1}^{DG}\le R_g^{up} \tag{22}$$

$$F_{g,t}=F_{g,t-1}-\frac{\Delta_t P_{g,t}^{DG}}{\eta_g^f FC_g H_g} \tag{23}$$

$$F_{g,t}\ge \underline{F}_g \tag{24}$$

$$\Pi_{g,t}\in\{0,1\}\quad \forall g\in\Omega_{DG} \tag{25}$$

where $P_{g,t}^{DG}$ is the active power emitted by the micro gas turbines units in the time period t of the node g. $Q_{g,t}^{DG}$ is the reactive power emitted by the micro gas turbines units in the time period t of the node g. $\overline{S}_g^{DG}$ is the maximum output power of the micro gas turbine units in a node g in a time period t. $\Pi_{g,t}$ is the binary variable of node g related to the micro gas turbine units in a time period t. When the micro gas turbine units are put into operation $\Pi_{g,t}=1$, and when the micro gas turbine units are not put into operation, $\Pi_{g,t}=0$. pf_g is the power factor limitation of the micro gas turbine units. R_g^{dw} is the falling limit of micro gas turbine units. R_g^{up} is the climbing limit of micro gas turbine units. $F_{g,t}$ is the remaining fuel (%) of micro gas turbine units. η_g^f is the fuel efficiency of the micro gas turbine units. FC_g is the fuel capacity of the micro gas turbine units. H_g is the calorific value of unit fuel of micro gas turbine units. $\underline{F}_g$ is the minimum fuel for the micro gas turbine units.

Similarly, the optimized microgrid system in this paper also includes energy storage devices. The constraints of energy storage systems are also a part that must be considered in the optimization process of microgrid systems. The energy storage system constraints are shown in Equations (26)–(32) [29, 33]:

$$SOC_{b,t}=\left(1-\xi_b\right)SOC_{b,t-1}-\frac{\Delta_t}{EC_b}\left(\frac{1}{\eta_b^{dc}}P_{b,t}^{ESS,dc}+\eta_b^{ch}P_{b,t}^{ESS,ch}\right) \tag{26}$$

$$\Phi_{b,t}\underline{P}_b^{dc}\le P_{b,t}^{ESS,dc}\le \Phi_{b,t}\overline{P}_b^{dc} \tag{27}$$

$$-\Lambda_{b,t}\underline{P}_b^{ch}\ge P_{b,t}^{ESS,ch}\ge -\Lambda_{b,t}\overline{P}_b^{ch} \tag{28}$$

$$\underline{SOC}_b\le SOC_{b,t}\le \overline{SOC}_b \tag{29}$$

$$SOC_b^{\tau}\le SOC_{b,t} \tag{30}$$

$$\Lambda_{b,t}+\Phi_{b,t}\le 1 \tag{31}$$

$$\Lambda_{b,t},\Phi_{b,t}\in\{0,1\}\quad \forall b\in\Omega_{ESS} \tag{32}$$

where $SOC_{b,t}$ is the state of charge of the energy storage system at a node b in a time period t. ξ_b is the self-discharge rate of the energy storage system at the node b. EC_b is the energy capacity of the energy storage system at the node b. η_b^{dc} is the discharge efficiency of the energy storage system at the node b. η_b^{ch} is the charging efficiency of the energy storage device at the node b. $\Phi_{b,t}$ is a binary variable related to the discharge operation of the energy storage system at the node b in the time period t. When discharged, $\Phi_{b,t}=1$. When charged, $\Phi_{b,t}=0$. $\underline{P}_b^{dc}$ is the minimum discharge power of an energy storage system. $\overline{P}_b^{dc}$ is the maximum discharge power of the energy storage device. $\Lambda_{b,t}$ is the binary variable related to the charging operation of the energy storage system. When charging, $\Lambda_{b,t}=1$. When discharging, $\Lambda_{b,t}=0$. $\underline{P}_b^{ch}$ is the minimum charging power of the energy storage system. $\overline{P}_b^{ch}$ is the maximum charging power of the energy storage system. $\underline{SOC}_b$ is the minimum state of charge of the energy storage system at a node b. $\overline{SOC}_b$ is the maximum state of charge of the energy storage system at a node b. SOC_b^{τ} is the minimum state of charge of the energy storage system at node b in the optimization period τ.

5 | SOLVING OPTIMIZATION MODEL BASED ON THE IMPROVED BENDERS ALGORITHM

The traditional Benders algorithm divides the optimization problem into sub-problems and main problems. Solving the sub-problems can get the upper bound of the original optimization problem. Solving the main problem can get the lower bound of the original optimization problem. The traditional Benders algorithm iteratively calculates the main and sub-problems until the main and sub-problems are less than a threshold.

This paper improves the traditional Benders algorithm. By improving the constraints of the main problem, the main problem can get a better lower bound result, which can speed up the algorithm convergence. The following details the improved Benders algorithm.

For the improved Benders algorithm, the objective function (16) and constraints in Section 3 need to be transformed into the form of a min-max-min standard model. The standard model of the improved Benders algorithm proposed in this paper is similar to the traditional Benders algorithm,

similar to that described in [33]. This paper will not go into details.

The improved Benders algorithm proposed in this paper is to deal with the two-stage robust optimization model of min-max-min. Similar to the traditional Benders algorithm, the improved Benders algorithm also needs to divide the optimization problem into sub-problems and the main problem. The sub-problem is used to deal with the optimization model of the max-min part, while the main problem is used to deal with the optimization model of the Min part. The process of dealing with the sub-problem needs to involve the dualization and linearization of the problem. The function of dualization in the sub-problem is to perform dual processing on the max-min part, so that the sub-problem is transformed into a problem of solving the maximum value. And then the upper bound of the original optimization problem is obtained. Since the nonlinear term of the variable will be generated in the process of dualization of the sub-problem, the nonlinear term also needs to be linearized. The sub-problem of the improved Benders algorithm proposed in this paper is the same as that of the traditional Benders algorithm, similar to that described in [33]. This paper will not go into details.

The improved Benders algorithm proposed in this paper improves the handling of the main problem. The process of dealing with the main problem will be elaborated below. The main purpose of the main problem is to optimize the decision variables z. The main problems with the Benders dual method are shown in Equations (33)–(36):

$$\min \xi = c^T z + \eta \tag{33}$$

$$Az \geq d \tag{34}$$

$$\eta \geq \left(b - Ez - Jw_l^*\right)^T \pi_l^* + \varsigma \quad \forall l \leq k \tag{35}$$

$$z \in S_z \tag{36}$$

where w_l^* is the result of the decision variable w obtained by solving the sub-problem. π_l^* is the result of the decision variable π obtained by solving the sub-problem. w_l^* and π_l^* are fixed-value parameters of the main problem. ς is the acceleration parameter. k is the number of iterations. Equation (33) is the objective function. Constraints include the constraints shown in Equation (34) of the decision variable z. Equation (35) is equivalent to the cut set generated by the subproblem.

Unlike the traditional Benders dual algorithm, the improved Benders dual algorithm proposed in this paper employs the acceleration parameter ς to the constraints of the main problem, as shown in Equation (35). The addition of acceleration parameter ς can makes the optimized result of the main problem larger. It can be seen from the simulation that the improved Benders algorithm proposed in this paper can accelerate the solution of the algorithm.

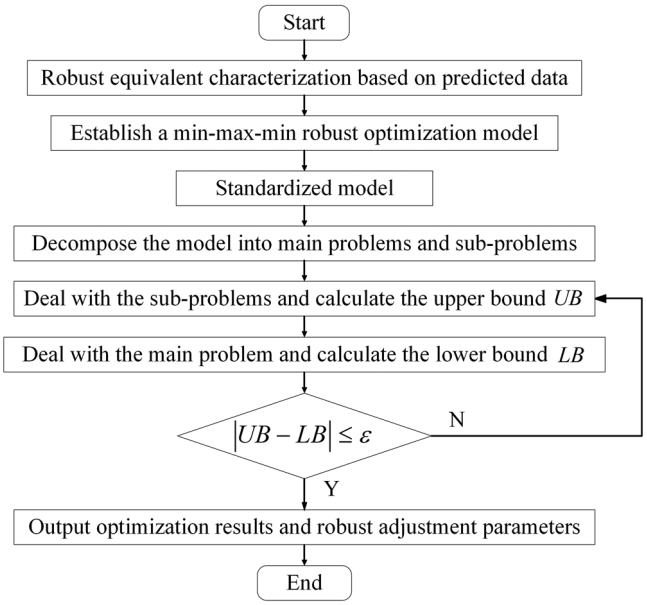

FIGURE 2 The overall flow chart of the improved Benders algorithm

Remark. The algorithm acceleration strategy proposed in this paper is to accelerate the Benders algorithm feedback link (Benders cut). By modifying the cuts generated by the sub-problem, as shown in Equation (35), the search range of the main problem is effectively reduced. The reduction of the search range of the main problem makes z obtained by the main problem closer to the final optimization result. Bringing this z^* into the sub-problem also makes w and π obtained by the sub-problem closer to the final optimization result. So we achieve the purpose of accelerating the solution speed of Benders algorithm. The larger the value of acceleration parameter ς is, the more obvious the influence of acceleration on the algorithm is. In order to satisfy the convergence of the algorithm, the value of ς has a range in general. The value range is shown in Equation (37):

$$0 < \varsigma < Q(z^*)_{\max} - Q(z^*)_{\min} \tag{37}$$

where $Q(z^*)_{\max}$ is the maximum value of $Q(z^*)$ during the algorithm iteration process. $Q(z^*)_{\min}$ is the minimum value of $Q(z^*)$ during the algorithm iteration process. The overall flow chart of the improved Benders algorithm is shown in Figure 2.

6 | SIMULATION ANALYSIS

6.1 | Simulation system and data

This paper uses a modified IEEE39-bus system [33] for simulation. The modified IEEE39 node system is shown in Figure 3. This paper is modelled in the MATLAB R2018a environment and calculated using the IBM CPLEX 12.8.0 solver.

Figure 4 shows the forecast data of uncertain factors such as photovoltaic output, wind turbine output and load demand. Figure 5 shows the price of electricity purchased by the microgrid

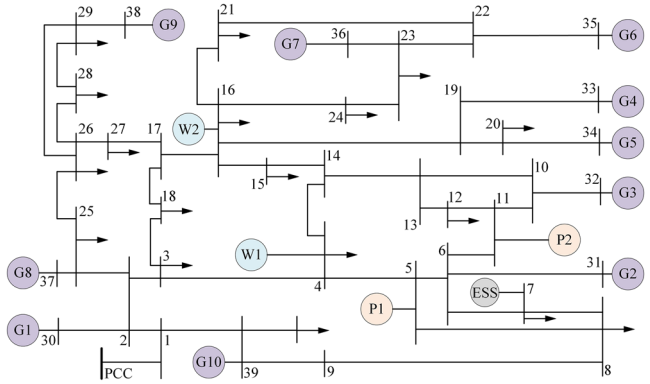

FIGURE 3 Modified IEEE39 node system

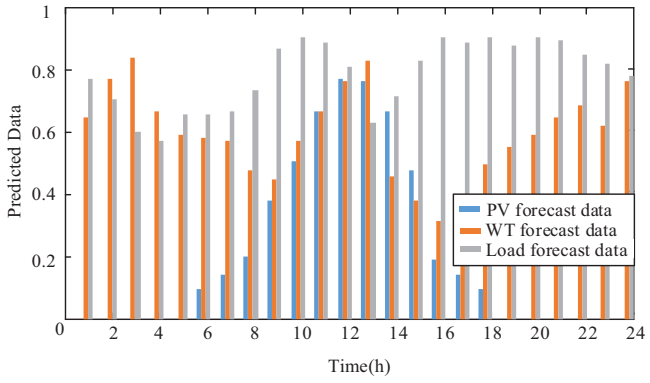

FIGURE 4 Forecasting data of photovoltaic output, wind turbine output and load demand

from the main grid and the unit price of traditional distributed power output.

6.2 | Grid-connected operation mode of microgrid

This section takes the scenario of a microgrid grid-connected operation mode as an example for simulation analysis. When the microgrid is connected to the grid, there is an electrical interaction between the microgrid and the main grid. When

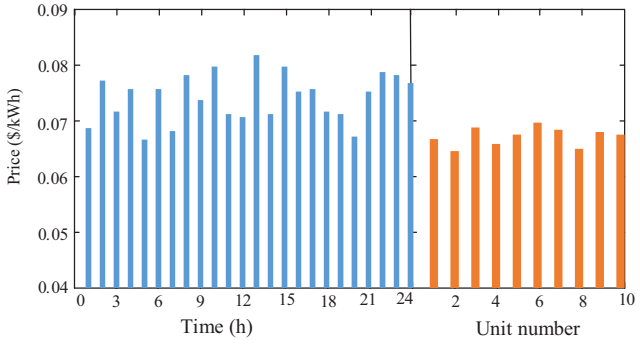

FIGURE 5 The unit price of electricity

TABLE 1 Microgrid operating costs in different small scenarios

Small scenarios	Operating costs ($)	Calculating time (s)
(a)	6.0828k	60.945558
(b)	7.3339k	58.422744
(c)	6.3871k	51.018100

the distributed power output in the microgrid is insufficient, the microgrid can purchase electricity from the main grid to meet the needs of the microgrid. When the output of renewable distributed power sources in the microgrid is too much, the microgrid cannot absorb the excess wind power and photovoltaic power generation. The microgrid can sell the surplus electricity to the main grid, thereby gaining profits and reducing the overall operating cost of the microgrid.

In order to better illustrate the advantages of the microgrid adaptive robust optimization model with different robust adjustment parameters proposed in this paper, this section compares the optimization results of three small scenarios. Small scenario (a) is a scenario based on the expectations of wind power, photovoltaics and load. This scenario is a scenario where robustness is not considered. Small scenario (b) is the worst scenario for wind power, photovoltaic and load. This scenario is a traditional robust optimization scenario. Small scenario (c) is the optimized scheduling model scenario proposed in this paper. In the simulation under the grid-connected operation mode of the microgrid, the acceleration parameter of the improved Benders algorithm adopted is $\varsigma = 0.2$. Table 1 shows the operating costs of the microgrid in three different small scenarios when the microgrid is connected to the grid.

It can be easily seen from Table 1 that the operating cost of the microgrid in the small scenario (c) is between the small scenario (a) and the small scenario (b). Small scenario (a) is a scenario that does not consider robustness, and only needs to perform optimal dispatch of the microgrid according to the predicted value of the uncertain factors. Because this small scenario is an ideal scenario, the operating cost of the microgrid in the small scenario (a) is less than the operating cost of the microgrid in the small scenario (c). But compared to the small scenario (a), when the output of the renewable distributed power generation is lower than the predicted value and the load demand is higher than the expectation, the optimized dispatch result of the small scenario (c) can still ensure the safe and stable operation of the microgrid. The small scenario (c) can ensure the robustness of microgrid operation. The small scenario (b) is the optimized dispatch result of the microgrid obtained by the traditional robust optimization, and is the optimized result under the worst scenario of uncertain factors. Because the optimization result of this small scenario is conservative, the operating cost of the microgrid in the small scenario (b) is greater than the operating cost of the microgrid in the small scenario (c). Through the microgrid adaptive robust optimization model proposed in this paper, small scenario (c) optimizes the adaptive robust adjustment parameters of microgrid operation to ensure the economy and robustness of microgrid operation.

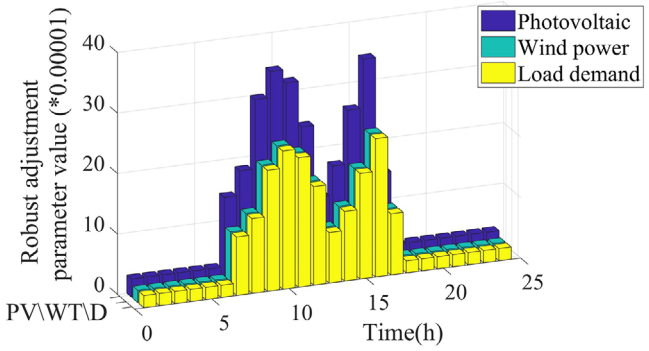

FIGURE 6 The changes of robust adjustment parameters ζ_{PV}, ζ_{WT} and ζ_D

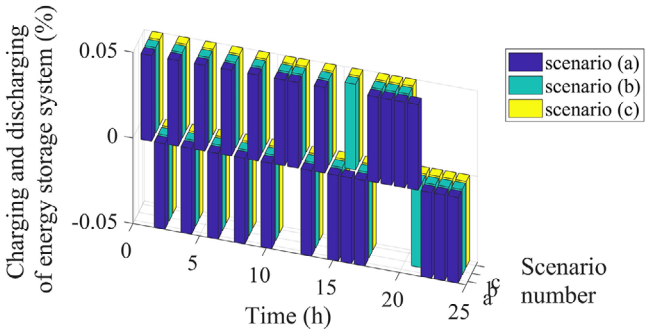

FIGURE 7 Charging and discharging of the energy storage system under three different small scenarios

Among them, for different uncertain factors, this paper obtains different adjustment coefficients through optimization. The adjustment coefficients are $Y_{PV} = 0.3$, $Y_{WT} = 0.2$ and $Y_D = 0.2$. The corresponding robust adjustment parameter value changes with the forecast data. Figure 6 shows the changes in robust adjustment parameters ζ_{PV}, ζ_{WT} and ζ_D. Robust adjustment parameters can reflect the robustness of the microgrid. Robust adjustment parameters can also effectively balance the economy and robustness of microgrid operation. The robust optimization model proposed in this paper can minimize the operating cost of the microgrid on the premise that the microgrid has certain robustness. The robustness adjustment parameters optimized according to different uncertain factors make the optimization results of the optimization model proposed in this paper more in line with the actual situation.

The charging and discharging conditions of the energy storage system in small scenarios (a), (b) and (c) are shown in Figure 7.

It can be seen from Figure 7 that the charging and discharging times of the energy storage system in the worst scenario are the same as the charging and discharging times of the energy storage system in the robust optimization scheduling scenario mentioned in this paper. The number of charge and discharge conversions of the energy storage system is 17 times. In the ideal scenario, without considering robustness, the energy storage system has fewer charge and discharge times, and the charge and discharge times are 15 times. The reason is that the energy

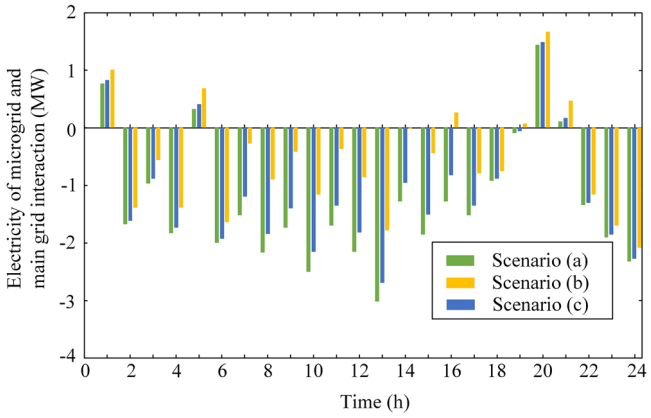

FIGURE 8 Energy interaction between microgrid and main grid

storage system of the microgrid requires more charging and discharging times to ensure that the microgrid can still operate stably even when uncertain factors deviate from the ideal state. Fewer charge-discharge conversion times are beneficial to the maintenance of the energy storage system. Reducing the maintenance cost of the energy storage system is also reduces the overall operating cost of the microgrid. When the output of renewable distributed energy sources such as photovoltaics and wind power is less than the expectation or the load demand is greater than the expectation, it may not be able to operate safely and stably, because the microgrid is not robust. In the 24 h scheduling process, the charge and discharge capacity of the energy storage system are the same, which indicates that the beginning and end states of the energy storage system are the same, and meets the requirements of the energy storage system charge and discharge constraints.

Figure 8 shows that the microgrid purchases electricity from the main grid or sells electricity to the main grid in three different small scenarios. The negative electricity exchange between the microgrid and the main grid means that the microgrid sells electricity to the main grid. The electricity interaction between the microgrid and the main grid is positive, which means that the microgrid purchases electricity from the main grid.

When the microgrid purchases electricity from the main network (such as 1 h, 5 h, 20 h, 21 h), the electricity purchased from the main network in scenario (c) is between the electricity purchased from the main network in scenario (a) and scenario (b). For the small scenario (b), due to the conservativeness of the traditional robust optimization on the estimation of uncertain parameters, the microgrid needs to purchase more power from the main grid. The microgrid purchases more electricity to ensure the safe and stable operation of the microgrid in the worst scenarios. In scenario (a), the corresponding microgrid purchases the smallest amount of electricity from the main grid, because it only considers the expectation of the uncertainty factors. But there is no robustness in actual operation in scenario (a).

At other times, the microgrid sells the remaining power to the main grid. It can be seen from Figure 8 that the electricity sold to the main network in the small scene (c) is between the

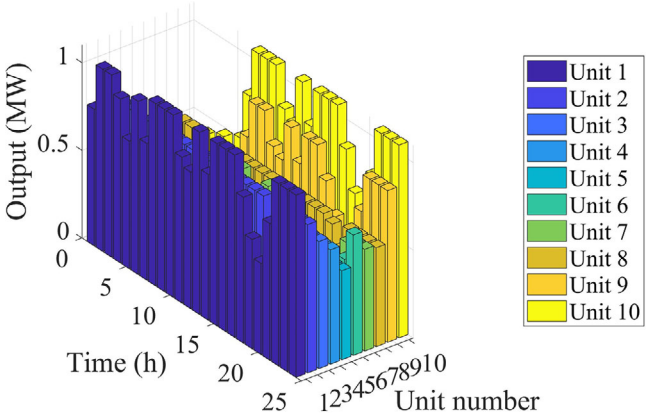

FIGURE 9 Traditional distributed power output of Grid-connected microgrid

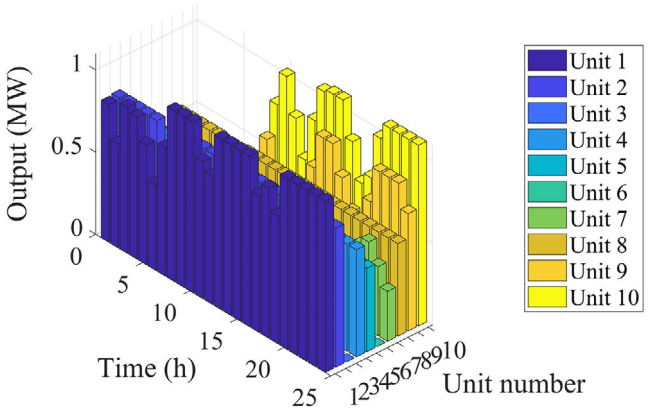

FIGURE 10 Traditional distributed power output of island microgrid

TABLE 2 Operating costs of microgrid under island and grid-connected mode

Operating status of microgrid	Operating costs ($)	Calculating time (s)
Island mode	6.9700k	69.898281
Grid-connected mode	6.3871k	51.018100

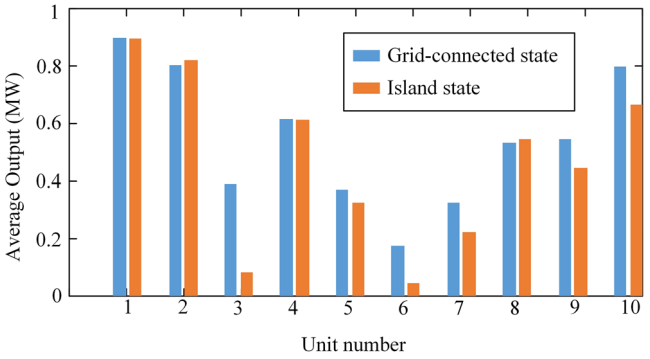

FIGURE 11 Comparison of average output

small scene (a) and the small scene (b). The reason is also similar to the reason why the microgrid purchases electricity from the main grid previously analyzed. Due to the sufficient output of renewable distributed energy sources such as photovoltaics and wind power, the microgrid can sell electricity to the main grid. In the worst scenario, the output of renewable distributed energy is lower than expected, so the microgrid sells the least amount of electricity to the main grid.

After the optimization of the robust optimization scheduling model proposed in this paper, the output of 10 traditional distributed power sources (micro gas turbine units) is shown in Figure 9.

6.3 | Island operation mode of microgrid

The microgrid cannot interact with the main grid for energy when it is operating in island mode. A microgrid needs to balance supply and demand within itself. In the simulation under the microgrid island operation mode, the acceleration parameter of the improved Benders algorithm adopted is $\varsigma = 0.2$. Table 2 shows the comparison of operating costs in the island mode and the grid-connected mode of the microgrid.

The adjustment coefficients obtained during islanding operation optimization are $Y_{PV} = 0.3$, $Y_{WT} = 0.3$ and $Y_D = 0.2$. Through the comparison, it is obvious that the operating cost in island mode is greater. Referring to Figure 8, in the process of interaction between the microgrid and the main grid in grid-connected mode, the microgrid sells electricity to the main network during most periods. When the microgrid is operating in island mode, the microgrid cannot sell excess electricity to the main grid. The microgrid cannot obtain profit from the electricity sold, and the corresponding operating costs are higher.

Figure 10 shows the output of 10 micro gas turbine units when the microgrid is operating in island mode. In order to clearly compare the output of traditional distributed power sources in grid-connected mode and the island mode of the microgrid, the average output of each traditional distributed power source in 24 h is compared. Figure 11 shows the comparison of the average output of 10 micro gas turbine units in grid-connected mode and the island mode of the microgrid.

When the microgrid is operating in grid-connected mode, the average output of 10 micro gas turbine units is 0.55413 MW. When the microgrid is operating in island mode, the average output of 10 micro gas turbine units is 0.473614 MW. The output of micro gas turbine units in grid-connected mode is greater than that of the micro gas turbine units in island mode, as shown in Figure 11. The reason is that when the power consumption of the main grid is large, the electricity price of the microgrid selling electricity to the main grid is high. The microgrid can enable micro gas turbine units to send more electricity to the main grid when the electricity price is high, thereby reducing the overall operating cost of the microgrid.

In island mode, the microgrid has no energy interaction process with the main grid. It can be seen from Figure 9 that the total amount of electricity transferred from the microgrid to the main grid in the grid-connected mode is 1.14546 MW. In island

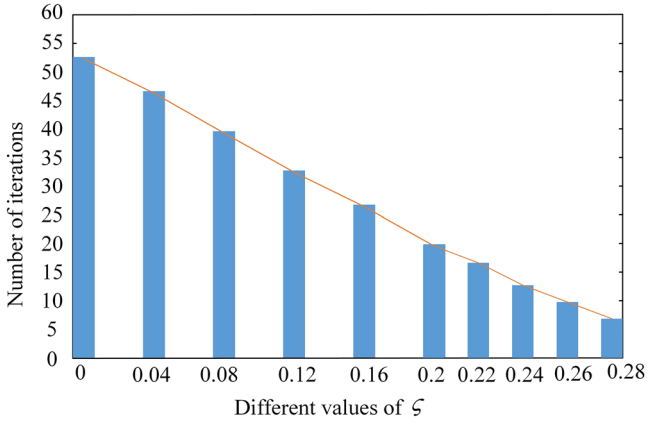

FIGURE 12 The number of iterations corresponding to different ς

mode, the traditional distributed power output of the microgrid is only reduced by 0.80516 MW. It shows that in order to ensure the robustness of the microgrid in island mode, there are situations such as abandoning wind and solar. It will cause energy waste and affect the economics of microgrid operations.

6.4 | Improved Benders duality algorithm

The improved Benders algorithm proposed in this paper achieves the purpose of accelerating the algorithm's solving speed by setting appropriate acceleration parameters ς. Figure 12 shows the number of algorithm iterations corresponding to different acceleration parameters ς in the microgrid grid-connected operation mode.

ς= 0 represents the traditional Benders dual algorithm. It can be seen from Figure 12 that the larger the value of the acceleration parameter ς, the smaller the number of iterations of the algorithm. The fewer the number of iterations, the less time is required for calculation and the higher the efficiency of the solution. The number of iterations of the algorithm changes linearly with the acceleration parameter ς. As the acceleration parameter ς increases, the number of iterations of the algorithm decreases significantly. When the acceleration parameter is ς= 0, the number of iterations of the algorithm is 53. When the acceleration parameter is ς = 0.28, the number of iterations of the algorithm is only 7. When the acceleration parameter value is larger, it will cause the solution to be impossible. The reason is that if the value of the acceleration parameter is too large, the lower bound of the original problem will be greater than the upper bound, and loop iteration cannot be performed. In order to better show the calculation efficiency of the improved Benders algorithm, the calculation time of the traditional Benders algorithm and the improved Benders algorithm when the acceleration factor ς = 0.2 is selected for comparison. The solution time of the traditional Benders algorithm is 160.864102s. The solution time of the improved Benders algorithm is 51.018100s. Compared with the traditional Benders algorithm, the improved Benders algorithm has increased the computational efficiency by 68.28%. The improved Benders algorithm effectively improves the solution efficiency of the traditional Benders algorithm.

The improved Benders dual algorithm proposed in this paper increases the solution result of the main problem. By increasing the lower bound of the loop, the upper and lower bounds of the Benders algorithm can reach the same value faster, and the final optimization result can be obtained faster.

7 | CONCLUSION

This paper proposes a microgrid adaptive robust optimal dispatch model with different robust adjustment parameters. The robust equivalent characterization method is used to convert uncertain parameters such as photovoltaic output, wind power output and load demand into corresponding definite parameters. Through optimization, different robust adjustment parameters for different uncertain parameters are obtained adaptively, which cannot only ensure the robustness of the microgrid, but also better ensure the economy. The robust adjustment parameters of different uncertain parameters are more in line with the actual conditions of microgrid operation. The establishment of a robust optimization model for microgrids can be applied to grid-connected and isolated operations of microgrids, and has more general applicability. Using the improved Benders algorithm to solve the established model can speed up the solution process and improve the efficiency of the solution. The adaptive robust optimization model of microgrids with different robust adjustment parameters proposed in this paper considers the robustness and economy of microgrid operation, and is more suitable for practical applications.

This paper studies the optimized operation of a single microgrid without considering the interconnection of multiple microgrids. In the future, research will be conducted on the optimal operation of microgrids under the condition of interconnected multiple microgrids.

ACKNOWLEDGEMENT

This work was supported in part by the National Key R&D Program of China (Grant No. 2018YFA0702200) and in part by the National Natural Science Foundation of China (Grant Number: 61773099).

ORCID

Jun Yang https://orcid.org/0000-0003-0599-1416

REFERENCES

1. Shi, Z.C., et al.: Multistage robust energy management for microgrids considering uncertainty. IET Gener. Transm. Distrib. 13(10), 1906–1913 (2019)
2. Vazquez, N., et al.: A fully decentralized adaptive droop optimization strategy for power loss minimization in microgrids with PV-BESS. IEEE Trans. Energy Convers. 34(1), 385–395 (2019)
3. Gupta, R.A., Gupta, N.K.: A robust optimization based approach for microgrid operation in deregulated environment. Energy Convers. Manage. 93, 121–131 (2015)
4. Zandi, F., et al.: Adaptive complex virtual impedance control scheme for accurate reactive power sharing of inverter interfaced autonomous microgrids. IET Gener. Transm. Distrib. 12(22), 6021–6032 (2018)

5. An, P.Q., et al.: Facilitating high levels of wind penetration in a smart grid through the optimal utilization of battery storage in microgrids: An analysis of the trade-offs between economic performance and wind generation facilitation. Energy Convers. Manage. 206, 112354 (2020)
6. Liu, G.D., Xu, Y., Tomsovic, K.: Bidding strategy for microgrid in day-ahead market based on hybrid stochastic/robust optimization. IEEE Trans. Smart Grid 7(1), 227–237 (2016)
7. Paul, T.G., et al.: A quadratic programming based optimal power and battery dispatch for grid-connected microgrid. IEEE Trans. Ind. Appl. 54(2), 1793–1805 (2018)
8. Taylor, J.W., Mcsharry, P.E., Buizza, R.: Wind power density forecasting using ensemble predictions and time series models. IEEE Trans. Energy Convers. 24(3), 775–782 (2009)
9. Talaat, M., et al.: Load forecasting based on grasshopper optimization and a multilayer feed-forward neural network using regressive approach. Energy 196, 117087 (2020)
10. Tewari, S., Geyer, C.J., Mohan, N.: A statistical model for wind power forecast error and its application to the estimation of penalties in liberalized markets. IEEE Trans. Power Syst. 26(4), 2031–2039 (2011)
11. Pinzon, J.A., et al.: Optimal management of energy consumption and comfort for smart buildings operating in a microgrid. IEEE Trans. Smart Grid 10(3), 3236–3247 (2019)
12. Luna, A.C., et al.: Mixed-integer-linear-programming-based energy management system for hybrid PV-wind-battery microgrids: Modeling, design, and experimental verification. IEEE Trans. Power Electron. 32(4), 2769-2783 (2017)
13. Liu, G., Tomsovic, K.: A full demand response model inco-optimized energy and reserve market. Electr. Power Syst. Res. 111, 62–70 (2014)
14. Zhang, Y., Wang, J., Zeng, B.: Chance-constrained two-stage unit commitment under uncertain load and wind power output using bilinear benders decomposition. IEEE Trans. Power Syst. 32(5), 3637–3647 (2017)
15. Luo, K., Shi, W.H., Wang, W.S.: Extreme scenario extraction of a grid with large scale wind power integration by combined entropy-weighted clustering method. Global Energy Interconnection 3(2), 140–148 (2020)
16. Peng, C.H., et al.: Flexible robust optimization dispatch for hybrid wind/photovoltaic/hydro/thermal power system. IEEE Trans. Smart Grid 7(2), 751–762 (2016)
17. Haddadian, H., Noroozian, R.: Multi-microgrids approach for design and operation of future distribution networks based on novel technical indices. Appl. Energy 185(1), 650–663 (2017)
18. Lv, T., Ai, Q.: Interactive energy management of networked microgrids-based active distribution system considering large-scale integration of renewable energy resources. Appl. Energy 163, 408–422 (2016)
19. Alipour, M., Zare, K., Seyedi, H.: A multi follower Bi-level stochastic programming approach for energy management of combined heat and power micro-grids. Energy 149(15), 135–146 (2018)
20. Ebrahimi, M.R., Amjady, N.: Adaptive robust optimization framework for day-ahead microgrid scheduling. Int. J. Electr. Power Energy Syst. 107, 213–223 (2019)
21. Zheng, Q.P., Wang, J., Liu, A.L.: Stochastic optimization for unit commitment a review. IEEE Trans. Power Syst. 30(4), 1913–1924 (2015)
22. Sang, B., et al.: Two-stage robust optimal scheduling of cooperative microgrids based on expected scenarios. IET Gener. Transm. Distrib. 14(26), 6741–6753 (2020)
23. Mohiti, M., et al.: Two-stage robust optimization for resilient operation of microgrids considering hierarchical frequency control structure. IEEE Trans. Ind. Electron. 67(11), 9439–9449 (2020)
24. Choi, J., et al.: Robust control of a microgrid energy storage system using various approaches. IEEE Trans. Power Syst. 10(3), 2702–2712 (2019)
25. Zhang, C., et al.: Multitimescale coordinated adaptive robust operation for industrial multienergy microgrids with load allocation. IEEE Trans. Ind. Inf. 16(5), 3051–3063 (2020)
26. Qiu, H.F., et al.: Robustly multi-microgrid scheduling: Stakeholder-parallelizing distributed optimization. IEEE Trans. Sustainable Energy 11(2), 988–1001 (2020)
27. Qiu, H.F., et al.: Recourse-cost constrained robust optimization for microgrid dispatch with correlated uncertainties. IEEE Trans. Ind. Electron. 68(3), 2266–2278 (2021)
28. Bian, Q., et al.: Distributional robust solution to the reserve scheduling problem with partial information of wind power. IEEE Trans. Power Syst. 30(5), 2822–2823 (2015)
29. Giraldo, J.S., et al.: Microgrids energy management using robust convex programming. IEEE Trans. Smart Grid 10(4), 4520–4530 (2019)
30. Zhang, C., et al.: Robust coordination of distributed generation and price-based demand response in microgrids. IEEE Trans. Smart Grid 9(5), 4236–4247 (2018)
31. Qiu, H.F., et al.: A historical-correlation-driven robust optimization approach for microgrid dispatch. IEEE Trans. Smart Grid 12(2), 1135–1148 (2021)
32. Zografou-Barredo, N.M., et al.: MicroGrid resilience-oriented scheduling: A robust MISOCP model. IEEE Trans. Smart Grid 12(3), 1867–1879 (2021)
33. Yang, J., Su, C.Q.: Robust optimization of microgrid based on renewable distributed power generation and load demand uncertainty. Energy 223, 120043 (2021)
34. Shams, M.H., et al.: Adjustable robust optimization approach for two-stage operation of energy hub-based microgrids. Energy 222, 119894 (2021)

How to cite this article: Yang, J., Su, C., Wang, Z.: Adaptive robust optimal dispatch of microgrid based on different robust adjustment parameters. IET Gener. Transm. Distrib. 15, 3360–3371 (2021). https://doi.org/10.1049/gtd2.12270